

# Synthesis, Characterization, and Catalytic Behavior of Ruthenium(II) Schiff Base Complexes

Scaffold A. Serron, Christopher M. Haar, and Steven P. Nolan\*

Department of Chemistry, University of New Orleans, New Orleans, Louisiana 70148

Lee Brammer

Department of Chemistry, University of Missouri, St. Louis, Missouri 63121-4499

Received July 14, 1997<sup>®</sup>

**Summary:** The complexes  $(X_6\text{-acen})\text{Ru}(\text{PPh}_3)_2$  ( $X = \text{H}$  (**1**) and  $\text{F}$  (**2**)) have been prepared and characterized by standard spectroscopic and analytical methods. Additionally, the solid-state structure of **2** has been determined by single-crystal X-ray diffraction. Ligand exchange reactions involving the labile  $\text{Ru}-\text{PPh}_3$  bond are easily performed, and complex **1** serves as a catalyst precursor for the isomerization of 1-hexene.

## Introduction

Metal–chelate Schiff base complexes have played an important role in developing stereochemical models in main group and transition metal coordination chemistry, mainly due to their stability, ease of preparation, and structural variability.<sup>1</sup> The planarity of the  $\text{N}_2\text{O}_2$  ligand provides a means of creating a large vacant site, where coordination and catalytic chemistry can be carried out. Representative examples of such complexes are available throughout the transition metal series,<sup>1–4</sup> from the group 4 derivatives prepared in the laboratories of both Floriani<sup>2</sup> and Jordan<sup>3</sup> to the highly effective chiral (salen)Mn(III) catalysts developed by Jacobsen for asymmetric olefin epoxidation.<sup>4</sup> In view of the diverse chemistry possessed by these ligands, we undertook the synthesis of  $(X_6\text{-acen})\text{Ru}(\text{PPh}_3)_2$  ( $X = \text{H}$  (**1**),  $\text{F}$  (**2**)). Although complex **1** has been previously reported,<sup>5</sup> to our knowledge it has not yet been examined as a potential catalyst. At the same time, it provides an informative contrast to the novel fluorinated analog **2** in terms of coordination and catalytic chemistry.

## Experimental Section

**General Considerations.** All manipulations involving organoruthenium complexes were performed under inert atmospheres of argon or nitrogen using standard high-vacuum or Schlenk-line techniques or in a Vacuum Atmospheres glovebox containing less than 1 ppm of oxygen and water.

<sup>®</sup> Abstract published in *Advance ACS Abstracts*, October 15, 1997.

(1) Garnovskii, A. D.; Nivorozhkin, A. L.; Minkin, V. I. *Coord. Chem. Rev.* **1993**, *126*, 1–69.

(2) (a) Dell'Amico, G.; Marchetti, F.; Floriani, C. *J. Chem. Soc., Dalton Trans.* **1982**, 2197. (b) Mazzanti, M.; Rosset, J. M.; Floriani, C.; Chiesi-Villa, A.; Guastini, C. *J. Chem. Soc., Dalton Trans.* **1989**, 953. (c) Floriani, C. *Polyhedron* **1989**, *8*, 1717. (d) Cobrazza, F.; Solari, E.; Floriani, C.; Chiesi-Villa, A.; Guastini, C. *J. Chem. Soc., Dalton Trans.* **1990**, 1335.

(3) Tjaden, E. B.; Swenson, D. C.; Petersen, J. L.; Jordan, R. F. *Organometallics* **1995**, *14*, 371–386.

(4) (a) Zhang, W.; Loebach, J. L.; Wilson, S. R.; Jacobsen, E. N. *J. Am. Chem. Soc.* **1990**, *112*, 2801–2803. (b) Jacobsen, E. N.; Zhang, W.; Guler, M. L. *J. Am. Chem. Soc.* **1991**, *113*, 6703–6704. (c) Zhang, W.; Jacobsen, E. N. *J. Org. Chem.* **1991**, *56*, 2296–2298.

(5) Thornback, J. R.; Wilkinson, G. *J. Chem. Soc. Dalton Trans.* **1978**, 110–115.

Solvents, including deuterated solvents for NMR analysis, were dried by standard methods<sup>6</sup> and distilled under nitrogen or vacuum-transferred before use. NMR spectra were recorded using Varian Gemini 300 MHz or Varian Unity 400 MHz spectrometers and are reported in ppm relative to tetramethylsilane (<sup>1</sup>H) or 85%  $\text{H}_3\text{PO}_4$  (<sup>31</sup>P). Elemental analyses were performed by Oneida Research Services, Whitesboro, NY.

**(H<sub>6</sub>-acen)Ru(PPh<sub>3</sub>)<sub>2</sub> (1).** In the glovebox, a 100 mL flask of a swivel-frit assembly was charged with  $\text{Ru}(\text{PPh}_3)_3\text{Cl}_2^7$  (0.315 g, 0.329 mmol),  $\text{Na}_2(\text{H}_6\text{-acen})^3$  (0.111 g, 0.334 mmol), and THF (15 mL). The apparatus was removed from the glovebox and attached to a high-vacuum line. The solution was stirred at room temperature for 24 h and filtered. The wine red filtrate was concentrated to ca. 5 mL, and hexane (10 mL) was vacuum-transferred into the same flask. When the mixture was stirred, the product precipitated as an orange solid, which was collected on the frit, washed with hexane (5 mL), and then dried thoroughly *in vacuo*. Yield: 0.205 g (74%). <sup>1</sup>H NMR (THF-*d*<sub>6</sub>):  $\delta$  1.01 (s, 6 H, 1-methyl), 1.42 (s, 6 H, 3-methyl), 2.86 (s, 4 H, methylene), 3.69 (s, 2 H, vinyl), 7.15–7.44 (m, 30 H, phenyl). <sup>31</sup>P{<sup>1</sup>H} NMR (THF-*d*<sub>6</sub>):  $\delta$  36.9. Anal. Calcd for  $\text{C}_{48}\text{H}_{48}\text{N}_2\text{O}_2\text{P}_2\text{Ru}$ : C, 67.99; H, 5.71; N, 3.30. Found: C, 68.34; H, 5.52; N, 3.18.

**(F<sub>6</sub>-acen)Ru(PPh<sub>3</sub>)<sub>2</sub> (2).** In the glovebox, a 100 mL flask of a swivel-frit assembly was charged with  $\text{Ru}(\text{PPh}_3)_3\text{Cl}_2^7$  (0.800 g, 0.834 mmol) and  $\text{Na}_2(\text{F}_6\text{-acen})^3$  (0.375 g, 0.835 mmol). THF (60 mL) was vacuum-transferred onto the solids, and the reaction was stirred for 24 h to give a wine red solution. After filtration, the solvent was removed *in vacuo*. The resulting red powder was then dissolved in toluene (30 mL) and then layered with pentane (30 mL). Once diffusion was complete, red crystals had grown. The solution was then very slowly cooled to –35 °C to complete crystallization. The resulting crystalline product was cold filtered, washed with cold pentane (5 mL), and dried thoroughly under vacuum. Yield: 0.505 g (64%). <sup>1</sup>H NMR (THF-*d*<sub>6</sub>):  $\delta$  1.37 (s, 6 H, methyl), 2.97 (s, 4 H, methylene), 4.11 (s, 2 H, vinyl), 7.19–7.42 (m, 30 H, phenyl). <sup>31</sup>P{<sup>1</sup>H} NMR (THF-*d*<sub>6</sub>):  $\delta$  33.5. Anal. Calcd for  $\text{C}_{48}\text{H}_{42}\text{F}_6\text{N}_2\text{O}_2\text{P}_2\text{Ru}$ : C, 60.31; H, 4.43; N, 2.93. Found: C, 60.37; H, 4.37; N, 2.80.

**Isomerization of 1-Hexene with (H<sub>6</sub>-acen)Ru(PPh<sub>3</sub>)<sub>2</sub>.** In the glovebox, a 5 mm NMR tube fitted with a Teflon valve was charged with  $(\text{H}_6\text{-acen})\text{Ru}(\text{PPh}_3)_2$  (2.7 mg, 3.2  $\mu\text{mol}$ ). The tube was then interfaced to the high-vacuum line, and  $\text{C}_6\text{D}_6$  (~0.3 mL) was vacuum-transferred onto the solid, followed by 1-hexene (0.19 g, 2.3 mmol), for a final substrate:catalyst ratio of 720:1. The reaction was allowed to proceed at ambient temperature (20–22 °C), with periodic monitoring by <sup>1</sup>H NMR spectroscopy. The isomerization rate was determined from the time-dependent ratio change of terminal and internal olefinic signal intensities, with the solvent peak as an internal reference.

(6) Perrin, D. D.; Armarego, W. L. F. *Purification of Laboratory Chemicals*, 3rd ed.; Pergamon Press: Oxford, 1988.

(7) Hallman, P. S.; Stephenson, T. A.; Wilkinson, G. *Inorg. Synth.* **1975**, *14*, 3060.

**Table 1. Summary of Crystallographic Data for (F<sub>6</sub>-acen)Ru(PPh<sub>3</sub>)<sub>2</sub> (2)**

empirical formula	C <sub>48</sub> H <sub>42</sub> F <sub>6</sub> N <sub>2</sub> O <sub>2</sub> P <sub>2</sub> Ru
cryst dimens, mm	0.50 × 0.42 × 0.15
space group	P2 <sub>1</sub> /n
unit cell dimens	
<i>a</i> , Å	12.5107(3)
<i>b</i> , Å	20.8177(5)
<i>c</i> , Å	16.8031(2)
α, deg	90
β, deg	101.154(1)
γ, deg	90
<i>V</i> , Å <sup>3</sup>	4293.6(2)
<i>Z</i> , molecule/cell	4
density (calcd), g/cm <sup>3</sup>	1.479
temperature, K	193(5)
X-ray wavelength, Å	0.710 73
diffractometer	Siemens SMART CCD
monochromator	highly-ordered graphite crystal
scan type	<i>ω</i>
data collected	-6 ≤ <i>h</i> ≤ 18, -26 ≤ <i>k</i> ≤ 30, -25 ≤ <i>l</i> ≤ 6
θ range, deg	1.58–32.22
abs corr	semiempirical from equiv reflns
no. of reflns measd	13 183
no. of indep reflns	9400 ( <i>R</i> <sub>int</sub> = 0.034)
<i>R</i> <sub>F</sub>	0.045 (for 7173 data <i>F</i> > 4σ( <i>F</i> ))
<i>wR</i> ( <i>F</i> <sup>2</sup> )	0.109
<i>S</i> ( <i>F</i> <sup>2</sup> )	1.432
no. of parameters	550
residual density	
max e/Å <sup>3</sup>	0.508
min e/Å <sup>3</sup>	-0.490

**Table 2. Selected Bond Distances (Å) and Bond Angles (deg) for (F<sub>6</sub>-acen)Ru(PPh<sub>3</sub>)<sub>2</sub> (2)**

Bond Lengths <sup>a</sup>			
Ru–N(1)	2.020(2)	Ru–N(2)	2.024(2)
Ru–O(1)	2.081(2)	Ru–O(2)	2.105(2)
Ru–P(2)	2.383(7)	Ru–P(1)	2.393(7)
P(1)–C(21)	1.836(3)	P(1)–C(41)	1.828(3)
P(1)–C(31)	1.829(4)	P(2)–C(51)	1.835(3)
P(2)–C(61)	1.836(3)	P(2)–C(71)	1.846(3)
O(1)–C(2)	1.283(4)	O(2)–C(7)	1.289(4)
N(1)–C(4)	1.315(4)	N(1)–C(11)	1.465(4)
N(2)–C(9)	1.304(4)	N(2)–C(12)	1.474(4)
C(1)–F(12)	1.336(4)	C(1)–F(11)	1.330(5)
C(1)–F(13)	1.351(4)	C(2)–C(3)	1.368(5)
C(2)–C(1)	1.513(5)	C(3)–C(4)	1.432(5)
C(4)–C(5)	1.507(4)	C(6)–F(62)	1.319(4)
C(6)–F(63)	1.334(4)	C(6)–F(61)	1.339(4)
C(6)–C(7)	1.514(4)	C(7)–C(8)	1.373(4)
C(8)–C(9)	1.440(4)	C(9)–C(10)	1.516(4)
C(11)–C(12)	1.528(4)		
Bond Angles <sup>a</sup>			
P(1)–Ru–P(2)	171.23(3)	O(1)–Ru–O(2)	89.97(10)
N(1)–Ru–N(2)	83.68(12)	N(1)–Ru–O(1)	93.37(11)
N(2)–Ru–O(2)	93.13(10)	C(51)–P(2)–C(71)	105.31(16)
C(51)–P(2)–C(61)	101.62(17)	C(61)–P(2)–C(71)	100.30(16)
C(21)–P(1)–C(31)	101.17(16)	C(21)–P(1)–C(41)	102.56(18)
C(31)–P(1)–C(41)	103.11(18)	C(2)–C(3)–C(4)	128.14(39)
C(7)–C(8)–C(9)	127.22(37)	P(2)–Ru–O(1)	85.50(7)
P(1)–Ru–O(1)	87.54(7)	P(2)–Ru–O(2)	89.44(7)
P(1)–Ru–O(2)	85.23(7)	N(2)–Ru–P(2)	90.85(8)
N(2)–Ru–P(1)	96.38(8)		

<sup>a</sup> Numbers in parentheses are the estimated standard deviations.

**Structure Determination of (F<sub>6</sub>-acen)Ru(PPh<sub>3</sub>)<sub>2</sub>.** Data were collected at reduced temperature for a red plate of dimensions 0.50 × 0.42 × 0.15 mm using a Siemens SMART CCD area detector diffractometer. The structure was solved by direct methods and refined to convergence on all *F*<sup>2</sup> data by full-matrix least-squares using the SHELXTL suite of programs.<sup>8</sup> Data were corrected for absorption by semiempirical methods based upon symmetry equivalent data.<sup>8</sup> All

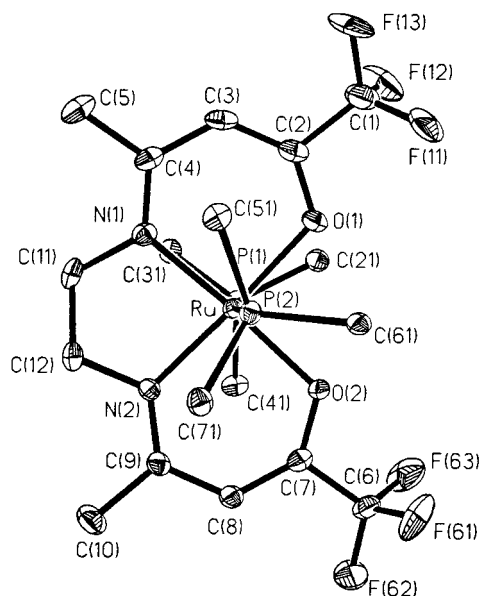
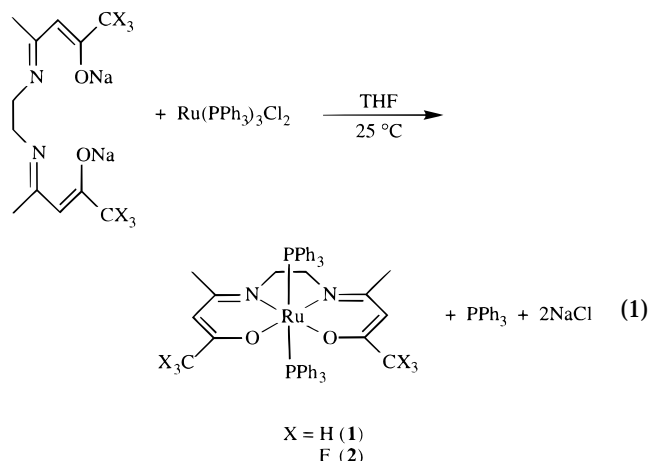


**Figure 1.** Molecular structure of (F<sub>6</sub>-acen)Ru(PPh<sub>3</sub>)<sub>2</sub> (2), with ellipsoids drawn in at 40% probability. Only the *ipso* carbons of the phenyl rings are shown.

non-hydrogen atoms were refined anisotropically; hydrogen atoms were included in calculated positions and refined using a riding model with fixed isotropic displacement parameters. Crystal data for (F<sub>6</sub>-acen)Ru(PPh<sub>3</sub>)<sub>2</sub> are summarized in Table 1, and selected bond lengths and angles are listed in Table 2. The ORTEP diagram in Figure 1 was drawn with ellipsoids at the 40% probability level.

## Results and Discussion

The title complexes can be synthesized in good yields by simple salt elimination from Ru(PPh<sub>3</sub>)<sub>3</sub>Cl<sub>2</sub> and Na<sub>2</sub>(X<sub>6</sub>-acen) in THF at ambient temperature, according to eq 1. The previously reported preparation of 1,<sup>5</sup> in

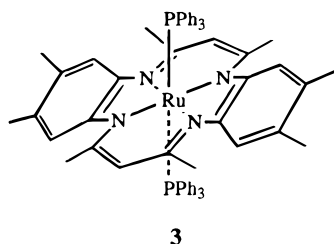


which the reaction is refluxed for several hours, offered significantly lower yields. In the solid state, the X = F complex is much more stable than the X = H derivative, the former being stable in air for weeks, the latter for less than 1 min. This trend also persists in solution, although oxidation occurs with much greater alacrity; solutions of either complex decompose within seconds of exposure to air.

These observations can be explained by examining the structural features of the complexes, as illustrated by the single-crystal X-ray diffraction determined structure

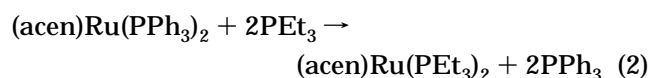
(8) SHELXTL-5.0, Siemens Analytical X-ray; Madison, WI, 1995.

of complex **2** (Figure 1). The ruthenium center is in a distorted octahedral geometry, with the equatorial positions occupied by the planar N<sub>2</sub>O<sub>2</sub>-chelate. The PPh<sub>3</sub> groups occupy the axial positions, with a slightly contracted P(1)–Ru–P(2) angle of 171.23(3)°. Even though the acyclic nature of the acen ligand affords a large opening for an incoming ligand, such as oxygen, by analogy to (omtaa)Ru(PPh<sub>3</sub>)<sub>2</sub> (**3**),<sup>9</sup> the stability of the present system in the solid state likely derives from an “umbrella” effect of the bulky PPh<sub>3</sub> ligands, which are canted toward the open space. The relative stability of



**1** and **2** may be a reflection of the differing electronic properties of the H<sub>6</sub>- and F<sub>6</sub>-acen moieties, the electron-withdrawing properties of the CF<sub>3</sub> substituents in the latter case rendering the Ru(II) center less sensitive to oxidation. In solution, however, oxidation of either complex is quite facile, suggesting that the Ru–phosphine interaction is easily disrupted by incoming ligands.

Indeed, the lability of the Ru–PPh<sub>3</sub> bonds in both **1** and **2** is illustrated by the ease with which PPh<sub>3</sub> is replaced by more basic, monodentate phosphines (eq 2).



The disappearance of coordinated PPh<sub>3</sub> signals in the <sup>31</sup>P NMR spectrum ( $\delta$  36.9, **1**;  $\delta$  33.5, **2**) is accompanied by the appearance of new signals at higher field ( $\delta$  21.1, **1**;  $\delta$  19.3, **2**) attributable to coordinated PEt<sub>3</sub> and the presence of free PPh<sub>3</sub> signals, indicating that all coordinated triphenylphosphine is substituted by added PEt<sub>3</sub>. Variations in the chemical shifts of the acen proton signals, in addition to the presence of two sets of ethyl signals (presumably coordinated and uncoordinated PEt<sub>3</sub>) are also consistent with such a process. Thornback and Wilkinson also postulated a similar process for the interaction of P(OMe)<sub>3</sub> with **1** based on <sup>1</sup>H NMR data.<sup>5</sup>

While the lability of the axial ligands in the present system suggests latent catalytic activity, the formation of mutually *cis* coordination sites is also required for the catalytically relevant addition–insertion–elimination sequence typical among the mid- and late-transition metals.<sup>10</sup> In this respect, the utilization of a Schiff base ligand is advantageous, as it leaves open one side of the equatorial plane, while the flexibility of an acyclic system should facilitate rearrangement of the supporting ligation, thus accommodating the necessary *cis* orientation. Complexes **1** and **2**, therefore, appeared to be promising candidates for certain types of catalytic transformations.

To investigate these possibilities, the isomerization of 1-hexene with **1** and **2** was carried out in C<sub>6</sub>D<sub>6</sub> at 20 °C. For complex **1**, the catalyst was able to complete a total of 500 turnovers, with an initial turnover frequency of 87 h<sup>–1</sup>. The same transformation was also attempted with **2** under identical conditions. After 3 days, however, there was only a small amount (<10%) of the isomerized product observed. The catalytic activity of **2**, therefore, more closely resembles that of (omtaa)Ru(PPh<sub>3</sub>)<sub>2</sub><sup>11</sup> in that neither complex appears particularly competent for 1-hexene isomerization in a nonpolar solvent such as benzene. In the (omtaa)Ru(PPh<sub>3</sub>)<sub>2</sub> case, this likely results from the need for ligand rearrangement in order to obtain *cis* coordination sites at which catalysis can occur. The rearranged structure, observed as a minor species in variable-temperature NMR experiments, should be more accessible through the use of highly polar solvents and elevated temperatures, and indeed, (omtaa)Ru(PPh<sub>3</sub>)<sub>2</sub> in methanol is a very effective catalyst for 1-hexene isomerization at 50 °C.<sup>11</sup> The reasons for the low activity of **2** for this transformation are not entirely clear. The same electron-withdrawing effect of the CF<sub>3</sub> groups which stabilizes the solid complex toward oxidation may also rob the Ru center of electron density, inhibiting abstraction of the substrate allylic proton,<sup>10</sup> a step implicitly required for the isomerization process. The presence of such an electronic effect is borne out by the shorter Ru–PPh<sub>3</sub> bond distances in **2** (2.393(7) and 2.383(7) Å) compared to those in (omtaa)Ru(PPh<sub>3</sub>)<sub>2</sub> (2.419(3) Å).<sup>11</sup> The shorter, presumably stronger, bond in **2** would be expected to increase the activation barrier to catalytically active species. The significant activity of complex **1**, on the other hand, provides a sharp contrast to the (omtaa)Ru(PPh<sub>3</sub>)<sub>2</sub> case. Even lacking the stabilizing effect of a polar solvent or the kinetic benefits of high temperature, a moderately fast turnover frequency was observed, suggesting that the combination of an open equatorial plane and flexible supporting ligation does in fact provide a promising template upon which to build a new catalytic system.

## Conclusion

The simple synthetic methodology described herein provides a convenient entry into the chemistry of ruthenium Schiff base complexes. The PPh<sub>3</sub> adducts are labile toward ligand substitution. Complex **1** is catalytically active for the isomerization of 1-hexene under mild conditions without requiring the use of highly polar solvents. The greater degree of flexibility of the supporting acen ligation in these complexes, as well as the opening an acyclic ligand system affords in the equatorial plane of the ruthenium coordination sphere, allows for the relatively easy formation of mutually *cis* coordination sites, leading to the observed catalytic activity in **1**. The electron deficiency of complex **2**, however, appears to inhibit the isomerization process. The efficiency of the synthetic procedures for both ligand and Ru complex preparations offers a promising range of catalytic systems, including those for asymmetric transformations. Current efforts aim to further exploit this potentially useful class of compounds.

(9) Luo, L. Ph.D. Thesis, University of New Orleans, 1995.

(10) Collman, J. P.; Hegedus, L. S.; Norton, J. R.; Finke, R. G. *Principles and Applications of Organotransition Metal Chemistry*; University Science Books: Mill Valley, CA, 1987.

(11) Luo, L.; Stevens, E. D.; Nolan, S. P. *Inorg. Chem.* **1996**, *35*, 252–254.

**Acknowledgment.** The National Science Foundation (Grant No. CHE-963116) and DuPont (Education Aid Grant) are gratefully acknowledged for support of this research. We thank Prof. Richard Jordan (University of Iowa) for helpful discussions. We are also indebted to Johnson Matthey/Aesar for generous loan of ruthenium salts.

**Supporting Information Available:** Tables of atomic coordinates, selected distances and angles, anisotropic thermal parameters, and hydrogen coordinates for **2** (7 pages). Ordering information is given on any current masthead page.

OM970600F